


Effective control and switching of optical multistability in a three-level V-type atomic systemAbdelsalam H. M. Abdelaziz^{1,2,*} and Amarendra K. Sarma^{1,†}¹*Department of Physics, Indian Institute of Technology Guwahati, Guwahati 781039, Assam, India*²*Department of Physics, Faculty of Science, Suez Canal University, Ismailia 41522, Egypt* (Received 4 May 2020; revised 9 September 2020; accepted 5 October 2020; published 30 October 2020)

We theoretically analyze the behavior of single optical bistability (OB), double OB, and tristability (OT) in a three-level V-type atomic system confined in a unidirectional optical ring cavity. The physics behind the emergence of various bistable and tristable states, and switching from the absorptive to the dispersive characteristics, are explored. The role of probe- and control-field detunings on the input-output characteristics is probed. Further, it is found that the switching between various bistable phenomena is defined by the ratio between the absolute peak values of the parameters describing dispersion and absorption, respectively. This ratio sets a criterion for obtaining absorptive OB, OT, double OB, and dispersive OB. The role of control-field intensity and detuning as well as the cooperation parameter on the input-output characteristics are explored. Finally, a scheme is discussed to control the width of the middle branch of double OB and OT as well as single OB.

DOI: [10.1103/PhysRevA.102.043719](https://doi.org/10.1103/PhysRevA.102.043719)**I. INTRODUCTION**

The possibility to modify linear absorption, dispersion, and nonlinearity of atomic medium ceaselessly pushes the research in optical sciences for half a century until now. Quantum coherence and interference, which led to the observation of the phenomena such as coherent population trapping (CPT) and electromagnetically induced transparency (EIT) are at the heart of manipulation of the properties of an atomic medium and have been studied extensively in past decades and continue to remain a major area of research in various contexts [1–12]. Among a plethora of phenomena, optical bistability (OB) and optical tristability (OT) have drawn much attention due to their numerous applications such as all-optical switching, optical transistors, optical memories, logical gates [13–16], and even in the context of cold atoms [17,18]. Initially, OB has been demonstrated experimentally for saturable absorber, ruby crystal, and sodium vapor as a nonlinear medium inside in an optical resonator [19–21]. Then, by developing the basic theoretical model of OB for two-level atoms coupled by a single-cavity mode [21–24], it was realized that OB arises due to intensity-dependent absorption or dispersion, or hybridization of both; henceforth, OB is classified as absorptive or dispersive or hybrid, respectively. A decade later, OT has been demonstrated for a Λ -type three-level atomic system comprising an excited state and two ground-state sublevels driven by two cavity modes [25–27]. Soon it was proposed that OB (OT) is more definitive with multilevel atoms than in two- (three-) level atoms as a nonlinear medium inside in an optical resonator. This is owing to the fact that absorption, dispersion, and nonlinearity could be greatly modified by quantum coherence

and interference in multilevel atoms for increased pathways. In this regard, coherent control by electromagnetic field-induced transparency (EIT) in three-level atomic systems was demonstrated theoretically and experimentally to reduce OB threshold intensity and give rise to a new type of OT by adjusting the control laser field parameters [28–30]. Also, by considering spontaneously generated coherence (SGC), the possibility of obtaining small cooperative parameter with low threshold intensity for OB and OT in three-level atomic systems was demonstrated [31–35]. Moreover, the optical bistability (OB) behavior of a three-level V-type atomic system inside a unidirectional ring cavity was demonstrated using a microwave field driving a hyperfine transition between two upper excited states. It was illustrated that, with the increase of the intensity of the coherent microwave driving field, the bistable threshold intensity increases and the hysteresis loop becomes wider [36]. Recently, incorporating coherent control by incoherent pumping in a Λ -type three-level atomic system was demonstrated to reduce OB threshold intensity [37]. Furthermore, hybrid absorptive-dispersive optical bistability (OB) behavior in an open Λ -type three-level atomic system by using a microwave field to drive the hyperfine transition between two lower states, along with the consideration of incoherent pumping and SGC, has been analyzed and demonstrated to reduce OB threshold intensity over a closed three-level atomic system [38]. On the other hand, the consideration of coherent control by incoherent pumping and SGC in an open Ξ -type three-level atomic system was shown to affect the OB threshold intensity, and give rise to OT by adjusting the detuning of the control laser field [39]. Alongside closed and open three-level schemes, four- and five-level atomic systems were proposed as promising alternatives to control OB and OT. In this context, considering SGC in a four-level atomic system was illustrated to decrease the threshold intensity for OB [40]. On the other hand, without considering SGC, OB and OT in an open and closed four-level atomic system inside

*ahm.abdelaziz@iitg.ac.in

†aksarma@iitg.ac.in

a standing-wave cavity were theoretically and experimentally studied [41,42]. Also, coherent control of nonlinear absorption of a probe field by both the coupling and control fields was shown to affect OB threshold intensity in Ξ -type four-level atomic system [43]. Moreover, coherent control of the two sublevels in the ground state was shown to manipulate the OB threshold intensity, and change OB to OT in an inverted Y-type four-level atomic system by switching the two orthogonally polarized cavity modes was reported [44]. Furthermore, coherent control by a microwave field driving two lower states and relative phase of the applied fields was demonstrated to control OB behavior, and change OB to OT in four-level systems [45,46]. Again, coherent control by the probe and the control field was shown to affect OB behavior, and switches OB to OT in a five-level EIT atomic system [47]. As previously mentioned, OB and OT in a three-level Λ -type atomic system have been extensively studied while less attention has been paid to investigate OB and OT in a three-level V-type atomic system. This may be owing to the coherence relaxation of upper levels by spontaneous emission which is not the case for Λ -type atomic system [31,48]. Hence, to the best of our knowledge, available studies on OB and OT in a three-level V-type atomic system are attempting to circumvent this effect by incorporating coherent control using incoherent pump field, or microwave field, or SGC [31–33,36,49–52]. In passing, it is worthwhile to note that various studies, including optical bistability, continues in V-type atomic systems. For example, very recently, experimental studies on optical bistability and nonlinear dynamics in a three-level V-type cold Yb-atomic system have been reported [53]. In this work, by assuming that a three-level atomic system should be sufficient for reliable obtainment of single OB, double OB, and OT, we investigate the criteria for achieving the same, without considering coherent control by incoherent pump field, or microwave field, or SGC. In addition, we propose a method to control the width of the middle branch of double OB and OT even at small cooperation parameter. We find that our proposed scheme for obtaining OB and OT in a three-level V-type atomic system, even amidst coherence relaxation of upper levels by spontaneous emission, is comparable or even better than that of ones reported with three-level Λ -type atomic system, where coherent control is done by making use of incoherent pump field, or microwave field, or SGC [15,16,28,29,34].

The paper is arranged as follows: In Sec. II we discuss the standard model for realizing single OB, double OB, and OT in a three-level V-type atomic system confined in a unidirectional ring cavity. Section III contains our simulated results and discusses the criteria for obtaining single OB, double OB, and OT in a V-type three-level atomic system, aside from the method for controlling the middle branch width of double OB and OT, followed by conclusions in Sec. IV.

II. MODEL

We consider a three-level V-type atomic system, as depicted in Fig. 1(a). The transition $|1\rangle \leftrightarrow |3\rangle$ with frequency ω_{31} is coupled by a coherent probe laser field of frequency ω_p and amplitude E_p . The transition $|1\rangle \leftrightarrow |2\rangle$ with frequency ω_c and amplitude E_c . The total electric field can be written

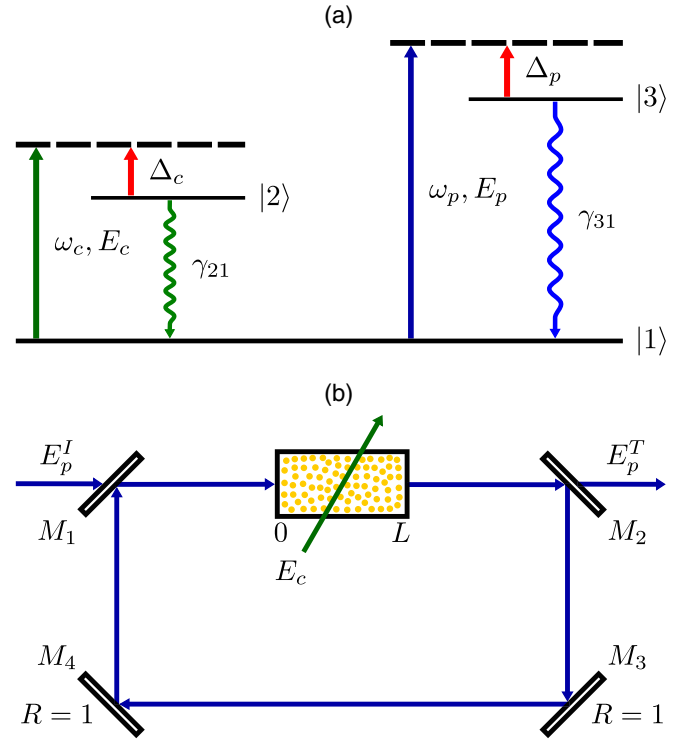


FIG. 1. (a) Three-level V-type atomic system, (b) unidirectional ring cavity.

as $\mathbf{E} = (\mathbf{E}_c e^{i\omega_c t} + \mathbf{E}_p e^{i\omega_p t} + \text{c.c.})/2$. Under the dipole and the rotating-wave approximations, the Hamiltonian of a three-level V-type atomic system is given by

$$\mathbf{H}/\hbar = \begin{bmatrix} 0 & \Omega_c^*/2 & \Omega_p^*/2 \\ \Omega_c/2 & -\Delta_c & 0 \\ \Omega_p/2 & 0 & -\Delta_p \end{bmatrix}, \quad (1)$$

where $\Omega_c = -\mu_{21}E_c/\hbar$ and $\Omega_p = -\mu_{31}E_p/\hbar$ are Rabi frequencies for the transitions with electric dipole moments μ_{21} and μ_{31} , respectively. $\Delta_c = \omega_c - \omega_{21}$ and $\Delta_p = \omega_p - \omega_{31}$ are the detunings of control and probe fields, respectively. It should be noted that $\omega_{ij} = \omega_i - \omega_j$. The density matrix equations describing the atomic system dynamics are given by

$$\begin{aligned} \dot{\rho}_{11} &= \gamma_{21}\rho_{22} + \gamma_{31}\rho_{33} - i[\Omega_c^*\rho_{21} + \Omega_p^*\rho_{31} - \text{c.c.}]/2, \\ \dot{\rho}_{22} &= -\gamma_{21}\rho_{22} + i[\Omega_c^*\rho_{21} - \text{c.c.}]/2, \\ \dot{\rho}_{33} &= -\gamma_{31}\rho_{33} + i[\Omega_p^*\rho_{31} - \text{c.c.}]/2, \\ \dot{\rho}_{21} &= \Gamma_{21}\rho_{21} - i[\Omega_c(\rho_{11} - \rho_{22}) - \Omega_p\rho_{23}]/2, \\ \dot{\rho}_{31} &= \Gamma_{31}\rho_{31} - i[-\Omega_c\rho_{32} + \Omega_p(\rho_{11} - \rho_{33})]/2, \\ \dot{\rho}_{32} &= \Gamma_{32}\rho_{32} - i[-\Omega_c^*\rho_{31} + \Omega_p\rho_{12}]/2 \end{aligned} \quad (2)$$

with $\rho_{ij} = \rho_{ji}^*$ and $\sum_{i=1}^3 \rho_{ii} = 1$. γ_{ij} denotes the spontaneous decay rate from state $|i\rangle$ to $|j\rangle$. $\Gamma_{21} = i\Delta_c - \gamma_{21}/2$, $\Gamma_{31} = i\Delta_p - \gamma_{31}/2$, and $\Gamma_{32} = i(\Delta_p - \Delta_c) - (\gamma_{21} + \gamma_{31})/2$.

In a unidirectional ring cavity, a three-level V-type atomic medium with number density N and length L is inserted as shown in Fig. 1(b). For simplicity, the mirrors M_3 and M_4 are assumed to be perfect, whereas $R(T)$ is the intensity reflection

(transmission) coefficient of mirrors M_1 and M_2 , provided that $R + T = 1$. The probe field E_p circulates in the cavity, while the control field E_c does not. The incident coherent probe field E_p^I entering the cavity through semisilvered mirror M_1 induces polarization $P(\omega_p)$ in the atomic medium and then transmitted partially from the mirror M_2 as E_p^T . Meanwhile, the control field can further modulate the induced polarization, which may modify the absorption and the dispersion of the atomic medium. Under the slowly varying envelope approximation and using Maxwell's equations, the equation describing the probe-field dynamics could be expressed as follows:

$$\frac{\partial E_p}{\partial t} + c \frac{\partial E_p}{\partial z} = \frac{i\omega_p}{2\epsilon_0} P(\omega_p), \quad (3)$$

where c is the speed of light, ϵ_0 is the permittivity of free space, and $P(\omega_p) = N\mu_{13}\rho_{31}$ is the slowly oscillating term for the induced polarization in the transition $|1\rangle \leftrightarrow |3\rangle$. It is worthwhile to note that it is possible to obtain an analytical expression for ρ_{31} , and thereby $P(\omega_p)$ [3,5,28]. The analytical expression for ρ_{31} is provided in the Appendix. However, rather than discussing this very complicated expression, we focus on our simplified model.

For a perfectly tuned ring cavity, in the steady-state limit, the boundary conditions between the incident field E_p^I and the transmitted field E_p^T are given by

$$E_p(L) = E_p^T / \sqrt{T}, \quad E_p(0) = \sqrt{T}E_p^I + RE_p(L). \quad (4)$$

By considering the mean-field limit, and employing the boundary conditions, the steady-state input-output relation for the probe field is written as [15,24,28]

$$y = x - iC\gamma_{31}\rho_{31}, \quad (5)$$

where $x = \mu_{13}E_p^T / (\hbar\sqrt{T})$ and $y = \mu_{13}E_p^I / (\hbar\sqrt{T})$ are the normalized output and input field, respectively, and $C = N\omega_p L \mu_{13}^2 / (2\hbar\epsilon_0 c T \gamma_{31})$ is the cooperation parameter. The input field y is complex while the transmitted amplitude x is assumed to be real [28].

The atomic system response to the applied fields is determined by the complex susceptibility parameter $\chi = \chi_R + i\chi_I$, which is connected to ρ_{31} , which is again a complex quantity, via the following relation:

$$\chi(\omega_p) = \frac{N\mu_{13}}{\epsilon_0 E_p} \rho_{31}(\omega_p). \quad (6)$$

It is well known that the real part of susceptibility, i.e., χ_R is related to dispersion while the imaginary one, i.e., χ_I , is related to absorption of the atomic system [54]. It is straightforward to show that

$$\chi_R = -\frac{N\mu_{13}}{C\gamma_{31}\epsilon_0 E_p} \text{Im}(y), \quad \chi_I = \frac{N\mu_{13}}{C\gamma_{31}\epsilon_0 E_p} [\text{Re}(y) - x]. \quad (7)$$

Thus, $\text{Im}(y)$ could be utilized to quantify dispersion, whereas $[\text{Re}(y) - x]$ could be used for enumeration of absorption. For the sake of brevity, in the rest of the work we will write $\chi' = \text{Im}(y)$ and $\chi'' = [\text{Re}(y) - x]$, and they could respectively be referred to as the real part of susceptibility and imaginary part of susceptibility in normalized units.

III. RESULTS AND DISCUSSIONS

We solve Eqs. (2) and their complex conjugates at the steady state, together with Eq. (5) numerically to study the input-output characteristics. As regards a real system, we may consider rubidium vapor as the cavity nonlinear medium to observe OB, double OB, and OT. The states $|1\rangle$, $|2\rangle$, and $|3\rangle$, respectively, refer to $5S_{1/2}$, $6P_{1/2}$, and $6P_{3/2}$ quantum states of Rb atoms. $\omega_{21}/2\pi = 113.18$ and $\omega_{31}/2\pi = 113.56$ THz are the transition frequencies with electric dipole moments $\mu_{21} = 2.7427$ and $\mu_{31} = 4.4342 \times 10^{-30}$ C m, respectively [55]. The corresponding spontaneous decay rates are $\gamma_{21}/2\pi = 0.23873$ and $\gamma_{31}/2\pi = 0.28170$ MHz [56]. The vapor cell length L could be taken as 0.05 m, and the intensity transmission coefficient T of mirrors M_1 and M_2 is 0.05. The cooperation parameter C is an adjustable parameter, and could be changed by varying the vapor density inside the cell. However, it is worthwhile to note that in order to set the cooperation parameter C to 100, the atomic number density N of $7 \times 10^{15} \text{ m}^{-3}$ is mandatory which corresponds to temperature ~ 292 K [57]. There is another possibility in which the probe and the control fields interchange their roles. In that case, $C = 100$ is possible at slightly higher atomic number density N of $6 \times 10^{16} \text{ m}^{-3}$ which corresponds to temperature ~ 300 K.

For the sake of brevity and to keep the calculations clean, in the rest of the work, we assume $\gamma_{21} = \gamma_{31}$ and scale all figures in the unit of γ_{31} . Figure 2 exhibits the effect of the probe field blue detuning Δ_p on the output field x as a function of the normalized parameters, the input field $|y|$, and the susceptibility components χ' and χ'' . It could be seen that for small Δ_p of $0.5\gamma_{31}$ [Fig. 2(a)], χ'' has a negative peak (absorption) at a small output field, while χ' after having a very small positive peak (positive refraction) at small output field, displays a negative peak (negative refraction) at intermediate output field. This feature may be used to explain the input-output characteristics, exhibiting OB, as shown by the blue-colored solid curve. Here, OB is of absorptive nature as its threshold intensity is mainly due to the absolute value of χ'' , at small output field. On the other hand, for large Δ_p of $2.6\gamma_{31}$ [Fig. 2(d)], χ'' exhibits a small negative peak value compared to the previous case. Interestingly, χ' does not show any initial positive peak unlike the previous case. Rather, it displays a minor negative peak at small output field followed by a small negative peak at an intermediate output field. This results in disappearance of absorptive OB at small output field and the emergence of dispersive OB, where the threshold intensity could be owing to the absolute value of χ' , at an intermediate output field.

In-between these two extreme cases, say, for Δ_p of $1.0\gamma_{31}$ [Fig. 2(b)], we find that χ'' has a negative peak at small output field, whereas χ' has a negative peak at intermediate output field. These features result in the formation of OT, as could be seen joining the higher and lower branches of absorptive and dispersive hysteresis loops, respectively, into a middle branch. In fact, we find that OT will exist whenever the width of the middle branch does not exceed the sum of respective widths of the lower and higher branches. It is worthwhile to note that OT could be changed to double OB by increasing Δ_p to $1.3\gamma_{31}$, as illustrated in Fig. 2(c). In this case, the width of the middle

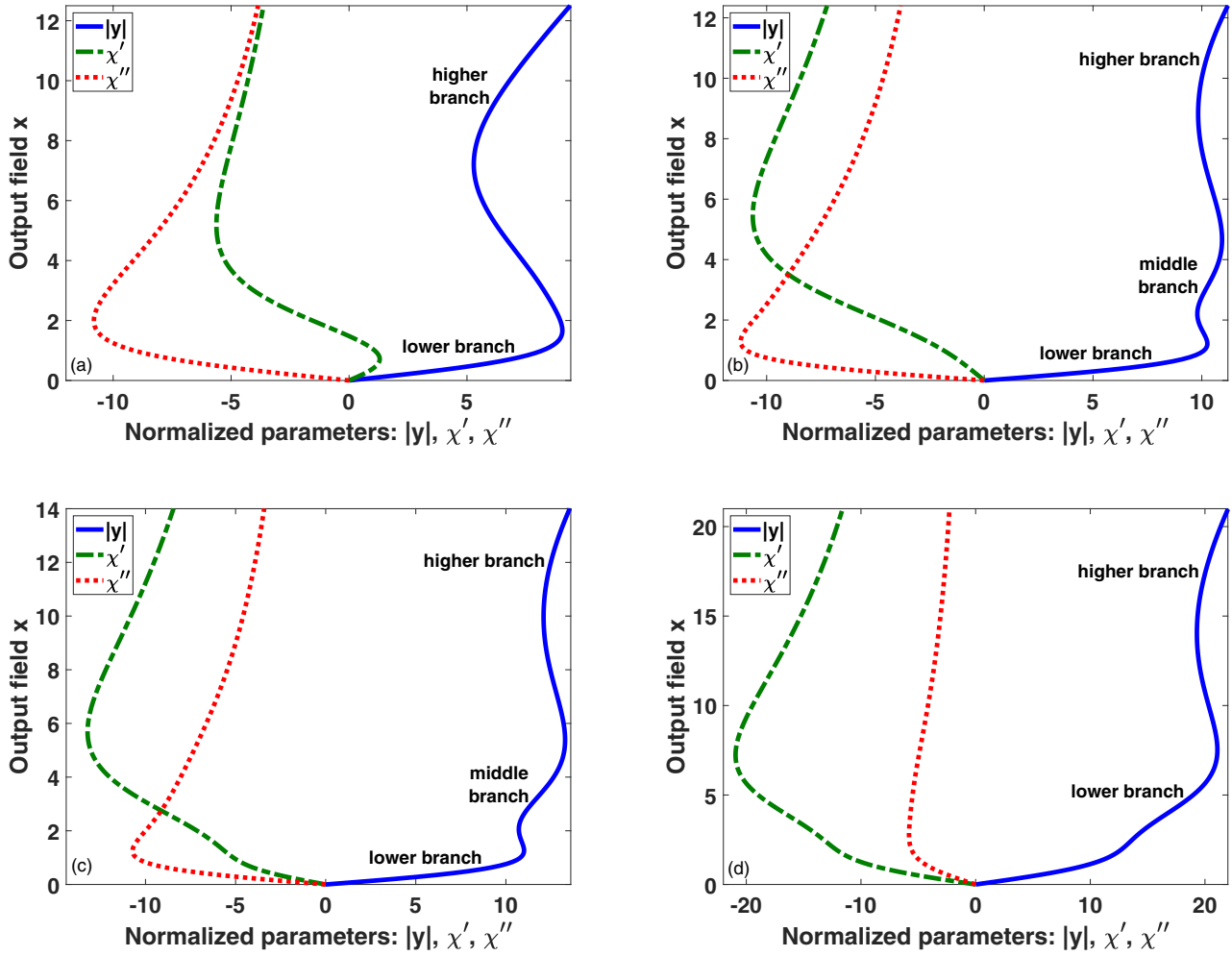


FIG. 2. Output characteristics as a function of the normalized parameters: the input field $|y|$ and the susceptibility components χ' and χ'' . For different values of probe-field detuning Δ_p/γ_{31} : (a) 0.5, (b) 1.0, (c) 1.3, and (d) 2.6. Other parameters are $\Delta_c = 0$, $\Omega_c = 2.2\gamma_{31}$, and $C = 100$.

branch exceeds the respective sum of the widths of the lower and higher branches. The difference between double OB and OT is that double OB has two stable output fields for each of two input field regions while OT has three stable output fields for one input field region. Moreover, the threshold intensities of the absorptive and dispersive hysteresis loops increase with probe field detuning.

Furthermore, it is revealed that the threshold intensities of the dispersive OB, and that of both OT and double OB, in the middle branch, are predominantly due to the absolute peak value of χ' at intermediate output field. On the contrary, the threshold intensities of absorptive OB and that of both OT and double OB, in the lower branch, are due to the absolute peak value of χ'' and/or χ' at small output field. Thus, it may be inferred that the ratio between the absolute peak value of χ' , at intermediate output field, and the absolute peak value of χ'' and/or χ' , at small output field, defines the switching between various bistable phenomena. If this ratio is considerably less than unity, absorptive OB is attainable and when it is around unity, OT could be obtained. On the other hand, if it is slightly more than unity, double OB is achievable, while if it is considerably more than unity, dispersive OB is

attainable. It is worthwhile to note that this ratio relies on the physical properties of the atomic system such as absorption and dispersion but not on the cavity feedback.

In Fig. 3 we show the effect of the control field detuning Δ_c on the behavior of single OB, double OB, and OT for a given blue-detuned probe field Δ_p . It is observed that, in Fig. 3(a), the hysteresis loop area of the absorptive OB could be enhanced by red detuning the control field, say, by $0.15\gamma_{31}$, compared to the case without detuning. This results in the increment of the threshold intensity of the lower branch, while reduction in the threshold intensity of the higher branch. On the other hand, blue detuning of the control field, by $0.15\gamma_{31}$, results in an increase of the threshold intensity in both the lower and the higher branches. Again, as illustrated in Figs. 3(b) and 3(c) respectively, we find that the absorptive and dispersive hysteresis loop area and width for both OT and double OB could be manipulated by detuning the control field. The threshold intensity of both the lower and middle branches gets affected while that of the higher branch remains almost the same. A similar effect could also be seen for the case with highly detuned probe field, as depicted in Fig. 3(d). However, in this case only the middle branch and the corresponding

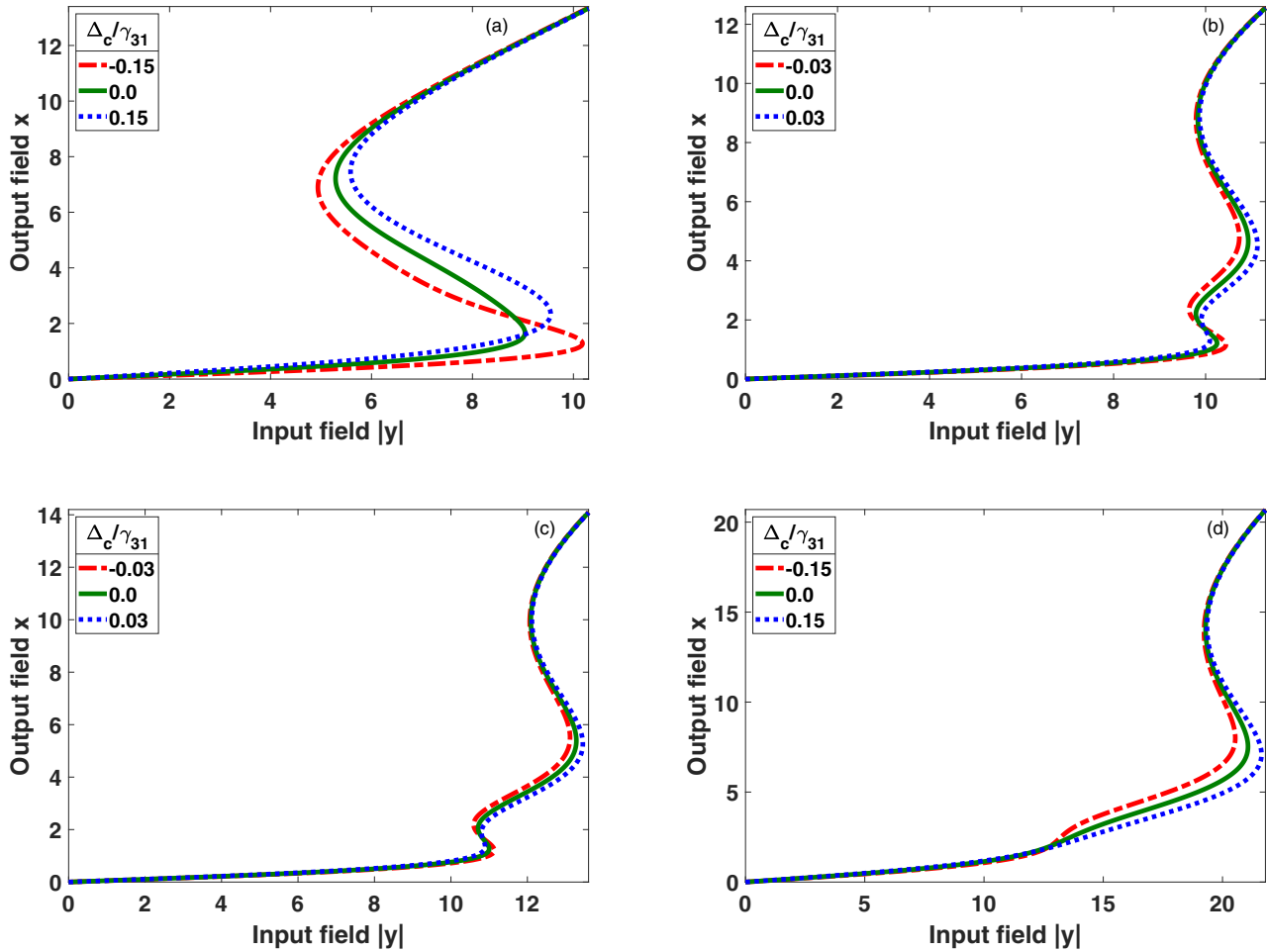


FIG. 3. Input-output characteristics under different control-field detunings Δ_c with blue detuning the probe field Δ_p/γ_{31} : (a) 0.5, (b) 1.0, (c) 1.3, and (d) 2.6. The remaining parameters are $\Omega_c = 2.2\gamma_{31}$ and $C = 100$.

threshold intensity could be engineered by detuning the control field. It is worth mentioning that for a given red-detuned probe field, the resonant control field results in the same input-output characteristics as that of the blue-detuned one. But in this case, detuning of the control field yields opposite effects, i.e., the blue-detuned control field exhibits the results shown by the red-detuned one with blue-detuned probe field and vice versa.

The effect of the control-field intensity Ω_c on the input-output characteristics, for a given detuned probe field, is illustrated in Fig. 4. It could be seen that for small Ω_c of $1.2\gamma_{31}$, only dispersive OB with very large area and width exists. However, as the control-field intensity Ω_c is increased to $2.0\gamma_{31}$ and $2.2\gamma_{31}$, emergence of OT and double OB could be observed. If Ω_c is increased to $3.0\gamma_{31}$, the unfolding of OB alone could be seen. Thus, it is possible to switch from dispersive OB to OT, double OB, and so on with judicious choice of the control-field intensity.

In Fig. 5 we show the effect of the cooperation parameter C on the input-output characteristics. It can be seen that, for small C of 75, only the absorptive hysteresis loop exists. Now, if C is increased to 100, the dispersive hysteresis loop emerges above the absorptive one. The threshold intensity of its lower branch is less than that of the middle branch, resulting in OT.

Further increment of C to 175 results in significant decrease in the absorptive hysteresis loop area, which is again situated

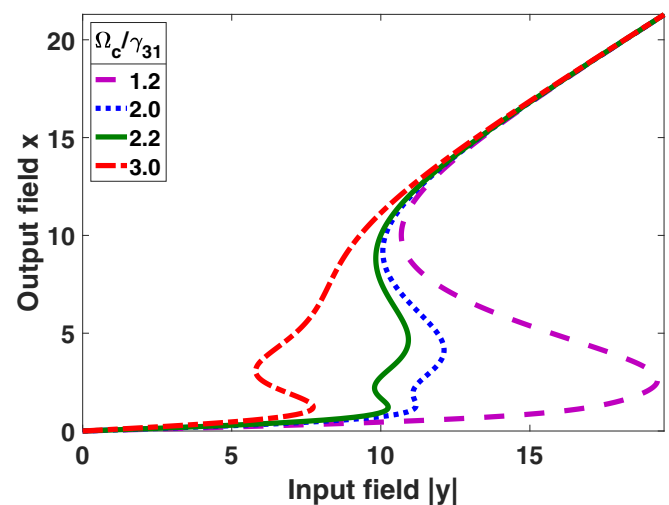


FIG. 4. Input-output characteristics under different control-field intensities Ω_c . Other parameters: $\Delta_p = 1.0\gamma_{31}$, $\Delta_c = 0.0\gamma_{31}$, and $C = 100$.

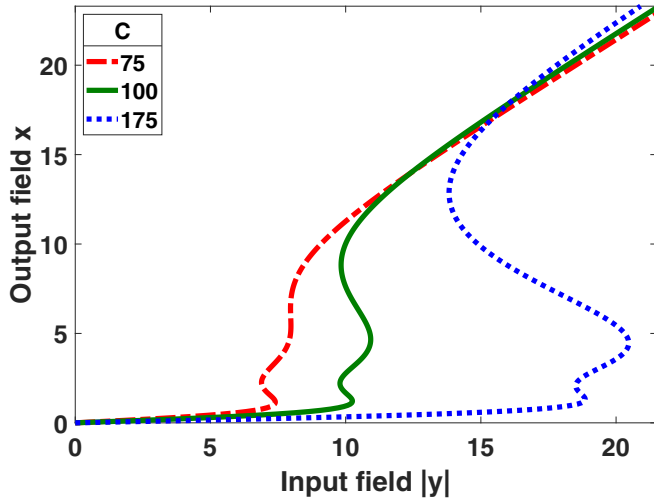


FIG. 5. Input-output characteristics under cooperation parameters C . Other parameters: $\Delta_p = 1.0\gamma_{31}$, $\Delta_c = 0.0\gamma_{31}$, and $\Omega_c = 2.2\gamma_{31}$.

below the dispersive hysteresis loop. It is easy to see that the required input threshold intensity to obtain OB or OT is significantly increased with higher C . Hence, the cooperation parameter needs to be chosen sagaciously. Finally, in what follows, we discuss the attainability of OT and double OB using a small control-field intensity Ω_c . In Fig. 6, we depict the combined effect of blue-detuned probe field and red-detuned control field on the input-output characteristics. Previously, we found that blue detuning the control field, for a given blue-detuned probe field, shrinks the absorptive hysteresis loop area, while the one for the dispersive case is increased. On the other hand, opposite effect could be observed by red detuning the control field, paving the way to control the width of the middle branch by adjusting the system parameters judiciously. Figure 6(a) exhibits dispersive OB, for a given blue-detuned probe field with $2.5\gamma_{31}$, if the control field is resonant. Now, if the control field is red detuned, say, by $0.9\gamma_{31}$, OT could be achieved. A slight increase in the detuning, say, to $1.0\gamma_{31}$, results in a smooth and wide OT characteristics. We find that in order to obtain double OB as well as OT, the probe-field detuning, i.e., Δ_p needs to be increased, along with the control-field detuning. This is clearly illustrated in Fig. 6(b). We observe that blue detuning the probe field by $3.6\gamma_{31}$ and red detuning the control field by $1.25\gamma_{31}$, unfolding of the double OB is achievable. Further increase in the detuning of the control field by $1.55\gamma_{31}$ gives rise to the ramification of OT. It may be noted that, while we have proposed atomic vapor as the nonlinear medium to observe OB, double OB, and OT, it may be possible to test the proposed scheme in other nonlinear systems as well. For example, asymmetric quantum wells, or double quantum dot nanostructure, or even a hybrid semiconductor quantum dot–metal nanoparticle system could possibly be modeled as a V-type system for the observation of the aforementioned phenomena [58–60]. It may be useful to note that SGC is extremely difficult to obtain in atomic systems. An effect similar to that, such as Fano-type interference, is possible in solid-state systems, which has been employed in Ref. [58]. Our work shows that even with such a type of

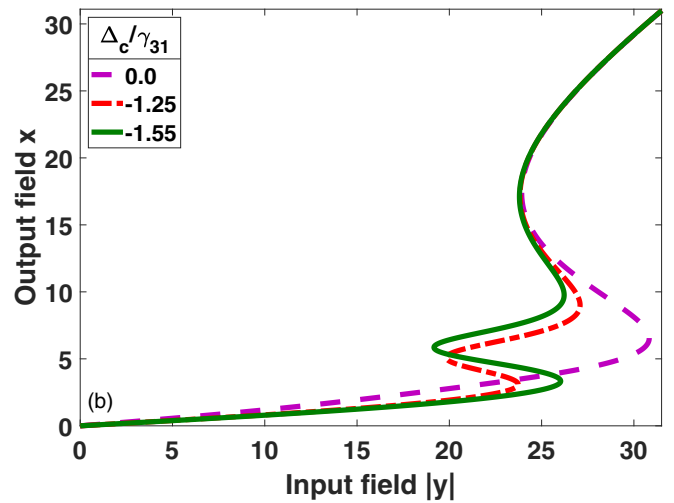
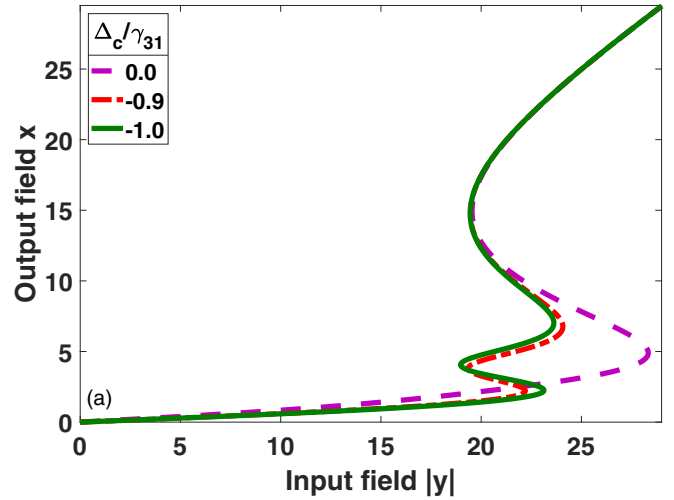


FIG. 6. Input-output characteristics under the combined effect of blue-detuned probe field and red-detuned control field. (a) $\Delta_p/\gamma_{31} = 2.5$ and (b) $\Delta_p/\gamma_{31} = 3.6$. Other parameters are $\Omega_c = 1.0\gamma_{31}$ and $C = 100$.

interference, while it reduces the threshold intensity, it is not mandatory to obtain OB, double OB, and OT.

IV. CONCLUSIONS

In conclusion, we have theoretically analyzed single OB, double OB, and OT behavior in a V-type three-level atomic system, confined in a unidirectional optical ring cavity. The work paves the ways to investigate the possibility of OB, double OB, and OT in a V-type system without considering coherent control by incoherent pump field, or microwave field, or SGC or Fano-type interference. Most importantly, we have tried to understand the physics behind the emergence of various bistable and tristable states, in particular switching from the absorptive to the dispersive characteristics. It is found that the switching between various bistable phenomena is defined by the ratio between the absolute peak values of the parameters describing dispersion and absorption, respectively. This ratio sets a criterion for obtaining absorptive OB, OT, double OB, and dispersive OB. It is interesting to note that this ratio

is independent of the cavity feedback. However, the respective width of the lower, the middle, and the higher branch of the hysteresis loop could be manipulated with judicious control of the detuning of the control and the probe fields. Further, we report that the threshold intensities of the absorptive and the dispersive hysteresis loops decrease with the control-field intensity but increase with the probe-field detuning and the cooperation parameter, thereby paving the way for easy control of the width of the middle branch of double OB and OT as well single OB. These results are crucial and useful for many

applications aiming toward fabrication of efficient all-optical switches and logic-gate devices for optical computing and quantum information processing.

ACKNOWLEDGMENT

A.H.M.A would like to thank Indian Council for Cultural Relations (ICCR), Government of India, and Ministry of Higher Education (MoHE), Egypt, for support through a research scholarship.

APPENDIX: ANALYTICAL FORM OF ρ_{31}

The steady-state solution for the off-diagonal density matrix element ρ_{31} is found to be the ratio of two polynomials of orders 5 and 6 in Ω_p :

$$\rho_{31} = 4\Omega_p \frac{\sum_{i=0}^2 [a_{2i} - i\gamma_{31}b_{2i}/2] |\Omega_p|^{2i}}{\sum_{i=0}^3 d_{2i} |\Omega_p|^{2i}}, \quad (\text{A1})$$

where a_{2i} , b_{2i} , and d_{2i} are real parameters that depend on probe- and control-field detunings, spontaneous decay rates, and control-field intensity. To arrive at the familiar expression for a two-level atomic system, simply set $i = 0$ and 1 in the numerator and denominator to retain the first-order term, and up to the second order in Ω_p , respectively, which result only in OB, while for a three-level atomic system, judicious choice of the system parameters plays the key role behind the emergence of OB, double OB, and OT. The detailed expressions for a_{2i} , b_{2i} , and d_{2i} parameters are given as follows:

$$a_0 = \Delta_p \gamma^m I_c^s (4\Delta^2 + \gamma_s^2) + 16\gamma^m (\Delta_c - \Delta) |\Omega_c|^4 + 4\gamma^m [\Delta_c (8\Delta\delta + \gamma_s^2) + \Delta_p (4\Delta^2 - \gamma_d \gamma_s)] |\Omega_c|^2, \\ a_2 = 16[\gamma_{21}^2 (\Delta_c - \Delta) + \gamma_{31}^2 \Delta_p] |\Omega_c|^2 + 8\gamma^m \Delta_p (4\Delta_c \Delta + \gamma_{21} \gamma_s), \quad a_4 = 16\gamma^m \Delta_p, \quad (\text{A2})$$

$$b_0 = \gamma^m I_c^s (4\Delta^2 + \gamma_s^2) + 16\gamma^m |\Omega_c|^4 + 4\gamma_{21} [-8\gamma_{31} \Delta_c \Delta + \gamma_s (4\Delta^2 + \gamma_s^2 - 2\gamma^m)] |\Omega_c|^2, \\ b_2 = 16(\gamma_s^2 - 2\gamma^m) |\Omega_c|^2 + 8\gamma^m (4\Delta_c \Delta + \gamma_{21} \gamma_s), \quad b_4 = 16\gamma^m, \quad (\text{A3})$$

$$d_0 = \gamma^m I_c^s I_p^s (4\Delta^2 + \gamma_s^2) + 128\gamma^m |\Omega_c|^6 + 16\gamma^m (I_c^s - 16\Delta_p \Delta + 4\gamma_{31} \gamma_s) |\Omega_c|^4 \\ + 8\gamma^m [I_c^s (4\Delta_c \Delta_p + \gamma^m + 2\gamma_{31}^2) + I_p^s (I_p^s - 8\Delta_c \Delta_p + 2\gamma^m)] |\Omega_c|^2, \\ d_2 = 128(\gamma_s^2 - \gamma^m) |\Omega_c|^4 + 32(3\gamma^m (4\Delta^2 + \gamma^m) - 4\Delta_c \Delta_p (\gamma_s^2 - 2\gamma^m) + 2\gamma^m (\gamma_s^2 - 2\gamma^m) + \gamma_{21}^2 (I_c^s + 2\Delta_p^2) \\ + \gamma_{31}^2 (I_p^s + 2\Delta_c^2)) |\Omega_c|^2 + 8\gamma^m [I_p^s (4\Delta_c \Delta_p + \gamma^m + 2\gamma_{21}^2) + I_c^s (I_c^s - 8\Delta_c \Delta_p + 2\gamma^m)], \\ d_4 = 128(\gamma_s^2 - \gamma^m) |\Omega_c|^2 + 16\gamma^m (I_p^s + 16\Delta_c \Delta + 4\gamma_{21} \gamma_s), \quad d_6 = 128\gamma^m, \quad (\text{A4})$$

where

$$\gamma_s = \gamma_{21} + \gamma_{31}, \quad \gamma_d = \gamma_{21} - \gamma_{31}, \quad \gamma^m = \gamma_{21} \gamma_{31}, \quad 2\delta = (\Delta_p + \Delta_c), \quad \Delta = (\Delta_p - \Delta_c), \\ I_p^s = (4\Delta_p^2 + \gamma_{31}^2), \quad I_c^s = (4\Delta_c^2 + \gamma_{21}^2). \quad (\text{A5})$$

-
- [1] G. Alzetta, A. Gozzini, L. Moi, and G. Orriols, *Nuovo Cimento B* **36**, 5 (1976).
[2] E. Arimondo and G. Orriols, *Lett. Nuovo Cimento* **17**, 333 (1976).
[3] F. T. Hioe and J. H. Eberly, *Phys. Rev. A* **25**, 2168 (1982).
[4] G. P. Zhang and T. F. George, *Phys. Rev. Lett.* **109**, 257401 (2012).
[5] G. P. Zhang, *J. Phys. B: At., Mol. Opt. Phys.* **46**, 035504 (2013).
[6] K.-J. Boller, A. Imamoglu, and S. E. Harris, *Phys. Rev. Lett.* **66**, 2593 (1991).
[7] M. D. Lukin and A. Imamoglu, *Nature (London)* **413**, 273 (2001).
[8] M. Fleischhauer, A. Imamoglu, and J. P. Marangos, *Rev. Mod. Phys.* **77**, 633 (2005).
[9] B. Dive, N. Koukoulekidis, S. Mousafeiris, and F. Mintert, *Phys. Rev. Res.* **2**, 013220 (2020).
[10] K. Hornberger, S. Gerlich, P. Haslinger, S. Nimmrichter, and M. Arndt, *Rev. Mod. Phys.* **84**, 157 (2012).
[11] S.-Y. Shiau and M. Combescot, *Phys. Rev. Lett.* **123**, 097401 (2019).
[12] B. Sarma and A. K. Sarma, *Phys. Rev. A* **96**, 053827 (2017).
[13] A. Brown, A. Joshi, and M. Xiao, *Appl. Phys. Lett.* **83**, 1301 (2003).

- [14] H. Chang, H. Wu, C. Xie, and H. Wang, *Phys. Rev. Lett.* **93**, 213901 (2004).
- [15] J. Sheng, U. Khadka, and M. Xiao, *Phys. Rev. Lett.* **109**, 223906 (2012).
- [16] J. Sheng, J. Wang, and M. Xiao, *Opt. Lett.* **38**, 5369 (2013).
- [17] B. Megyeri, G. Harvie, A. Lampis, and J. Goldwin, *Phys. Rev. Lett.* **121**, 163603 (2018).
- [18] E. V. Anikin, N. S. Maslova, N. A. Gippius, and I. M. Sokolov, *Phys. Rev. A* **100**, 043842 (2019).
- [19] A. Szöke, V. Daneu, J. Goldhar, and N. A. Kurnit, *Appl. Phys. Lett.* **15**, 376 (1969).
- [20] T. N. C. Venkatesan and S. L. McCall, *Appl. Phys. Lett.* **30**, 282 (1977).
- [21] H. M. Gibbs, S. L. McCall, and T. N. C. Venkatesan, *Phys. Rev. Lett.* **36**, 1135 (1976).
- [22] R. Bonifacio and L. A. Lugiato, *Phys. Rev. A* **18**, 1129 (1978).
- [23] A. T. Rosenberger, L. A. Orozco, H. J. Kimble, and P. D. Drummond, *Phys. Rev. A* **43**, 6284 (1991).
- [24] J. Wu, X.-Y. Lü, and L.-L. Zheng, *J. Phys. B: At., Mol. Opt. Phys.* **43**, 161003 (2010).
- [25] M. Kitano, T. Yabuzaki, and T. Ogawa, *Phys. Rev. Lett.* **46**, 926 (1981).
- [26] S. Cecchi, G. Giusfredi, E. Petriella, and P. Salieri, *Phys. Rev. Lett.* **49**, 1928 (1982).
- [27] C. M. Savage, H. J. Carmichael, and D. F. Walls, *Opt. Commun.* **42**, 211 (1982).
- [28] W. Harshawardhan and G. S. Agarwal, *Phys. Rev. A* **53**, 1812 (1996).
- [29] A. Joshi, A. Brown, H. Wang, and M. Xiao, *Phys. Rev. A* **67**, 041801(R) (2003).
- [30] A. Joshi and M. Xiao, *Phys. Rev. Lett.* **91**, 143904 (2003).
- [31] M. A. Antón and O. G. Calderón, *J. Opt. B* **4**, 91 (2002).
- [32] A. Joshi, W. Yang, and M. Xiao, *Phys. Rev. A* **68**, 015806 (2003).
- [33] S. M. Mousavi, L. Safari, M. Mahmoudi, and M. Sahrai, *J. Phys. B: At., Mol. Opt. Phys.* **43**, 165501 (2010).
- [34] A. Joshi, W. Yang, and M. Xiao, *Phys. Lett. A* **315**, 203 (2003).
- [35] D.-c. Cheng, C.-p. Liu, and S.-q. Gong, *Phys. Lett. A* **332**, 244 (2004).
- [36] J. Li, *Phys. D (Amsterdam)* **228**, 148 (2007).
- [37] H. Jafarzadeh, M. Sahrai, and K. Jamshidi-Ghaleh, *Appl. Phys. B* **117**, 927 (2014).
- [38] Z. Wang, A.-X. Chen, Y. Bai, W.-X. Yang, and R.-K. Lee, *J. Opt. Soc. Am. B* **29**, 2891 (2012).
- [39] S. H. Asadpour, H. R. Hamed, and H. R. Soleimani, *J. Mod. Opt.* **60**, 659 (2013).
- [40] L. Xin-You, L. Jia-Hua, L. Ji-Bing, and L. Jin-Ming, *J. Phys. B: At., Mol. Opt. Phys.* **39**, 5161 (2006).
- [41] A. Sharma, T. Ray, R. V. Sawant, G. Sheikholeslami, S. A. Rangwala, and D. Budker, *Phys. Rev. A* **91**, 043824 (2015).
- [42] R. Sawant and S. A. Rangwala, *Phys. Rev. A* **93**, 023806 (2016).
- [43] P. Kumar and S. Dasgupta, *Phys. Rev. A* **94**, 023851 (2016).
- [44] S. Hossein Asadpour and A. Eslami-Majd, *J. Lumin.* **132**, 1477 (2012).
- [45] A. Vafafard, H. Zaakeri, L. E. Zohravi, and M. Mahmoudi, *J. Opt. Soc. Am. B* **31**, 1981 (2014).
- [46] X. Hu, H. Zhang, H. Sun, Y. Lei, H. Li, and W. Liu, *Appl. Opt.* **55**, 6263 (2016).
- [47] D. X. Khoa, L. V. Doai, L. N. Mai Anh, L. C. Trung, P. V. Thuan, N. T. Dung, and N. H. Bang, *J. Opt. Soc. Am. B* **33**, 735 (2016).
- [48] D. Walls, P. Zoller, and M. Steyn-Ross, *IEEE J. Quantum Electron.* **17**, 380 (1981).
- [49] M. Antón, O. G. Calderón, and F. Carreño, *Phys. Lett. A* **311**, 297 (2003).
- [50] K. I. Osman, *Opt. Commun.* **259**, 194 (2006).
- [51] Z. Wang and M. Xu, *Opt. Commun.* **282**, 1574 (2009).
- [52] Y.-N. Li, Y.-Y. Chen, and R.-G. Wan, *J. Opt. Soc. Am. B* **36**, 1799 (2019).
- [53] H. Gothe, T. Valenzuela, M. Cristiani, and J. Eschner, *Phys. Rev. A* **99**, 013849 (2019).
- [54] R. W. Boyd, *Nonlinear Optics*, 4th ed. (Academic, Hoboken, NJ, 2020).
- [55] C. D. Herold, V. D. Vaidya, X. Li, S. L. Rolston, J. V. Porto, and M. S. Safronova, *Phys. Rev. Lett.* **109**, 243003 (2012).
- [56] J. E. Sansonetti, *J. Phys. Chem. Ref. Data* **35**, 301 (2006).
- [57] C. B. Alcock, V. P. Itkin, and M. K. Horrigan, *Can. Metall. Q.* **23**, 309 (1984).
- [58] D. Sun, H. Zhang, and H. Sun, *J. Phys. B: At., Mol. Opt. Phys.* **52**, 035501 (2019).
- [59] Z. Wang and B. Yu, *J. Opt. Soc. Am. B* **30**, 2915 (2013).
- [60] G. Solookinejad, M. Jabbari, M. Nafar, E. Ahmadi, and S. H. Asadpour, *J. Appl. Phys.* **124**, 063102 (2018).